



Synthesis and Tumor Targeting Evaluation of new radiopharmaceuticals based on vanillin and gallic acid derivatives for tumor imaging

Samar A. Ibrahiem^{1*}, Yara E. Mansour², Tamer M. Sakr³, Wafaa A. Zaghary¹

¹Pharmaceutical chemistry department, faculty of pharmacy, Helwan University, Egypt. ²Pharmaceutical organic chemistry department, faculty of pharmacy, Helwan University, Egypt. ³Radioactive Isotopes and Generator Department, Hot Labs Center, Egyptian Atomic Energy Authority, PO13759, Cairo, Egypt *Corresponding author: Yara E. Mansour (Yara_masnour@pharm.helwan.edu.eg)

Received: 1 May 2025 Revised: 30 May 2025 Accepted: 13 June 2025 Published: 29 October 2025

Egyptian Pharmaceutical Journal 2025, 24: 160-

Background and objective

Radiopharmaceutical applications in tumor imaging are widely used nowadays. Radioisotopes alone can not reach the tumor easily, so they can be linked with a carrier to deliver the radioisotope to the tumor site. These carriers could be peptides, antibodies or small chemical agents.

Materials and methods

In our study, gallic acid (GA) derivative **4** and vanillin derivative **6** were used as two targeting chemical agents to be linked with $[^{99m}Tc]$ to prepare $[^{99m}Tc]$ Tc-4 and $[^{99m}Tc]$ Tc-6, as 4 and 6 have a good pharmacokinetics properties compared to GA and vanillin respectively , also we designed these two derivative to be coupled with $[^{99m}Tc]$ as they rich with electron donating groups, these two radiopharmaceutical were injected into mice .

Results and conclusion

T/NT results were calculated for both of [99mTc] Tc-4 and [99mTc] Tc-6 after 15 min, 30 min, 60 min and 180 min. T/NT for [99mTc] Tc-4 and [99mTc] Tc-6 at 60 min was 1.74 and 4.32, respectively. Therfore, we can conclude that [99mTc] Tc-4 and [99mTc] Tc-6 have powerful targeting properties toward tumor cells , so that these two chemical agents **4** and **6** are promising to be applied in radiopharmaceutical applications.

Keywords: Radiopharmaceutical, radioisotope, radio-imaging, tumor, vanillin, gallic acid Egypt Pharmaceut J 24:160–174

© 2025 Egyptian Pharmaceutical Journal 1687-4315

Introduction

Cancer continues to be the leading cause of death worldwide. The the primary causes of death are drug resistance and the potential for metastasis to distant organs [1,2]. At this advanced stage, treatment options vary for each patient and may include radiotherapy, chemotherapy, hormone therapy, targeted therapy Radiopharmaceuticals are continually under development, as they facilitate the monitoring of tumor progression and response to therapy, or can even be used directly as treatment. Radio-imaging is a form of molecular imaging that involves the use of small chemical agents, antibodies, or peptides as carriers for medical diagnostic radioisotopes. Technetium-99m [99mTc] is widely used as a radioisotope for labeling various organic molecules to study their in vivo bio-distribution and evaluate pharmacokinetics. It is also used as a model for tumor radio-imaging [4-9] [99mTc] remains one of the most widely utilized radioisotopes in nuclear medicine, particularly for tumor imaging, due to its

favorable physical and chemical properties. Its physical half-life of approximately 6 hours is optimal for diagnostic imaging—it allows sufficient time radiopharmaceutical preparation, administration, and imaging, while minimizing the patient's radiation exposure [10]. From clinical use point of view; [99mTc] serves as the best diagnostic radionuclide for application due to its unique characteristics such as its gamma energy is 140 KeV which is well-suited for detection using gamma cameras, particularly in single-photon emission computed tomography (SPECT), ensuring high image resolution and diagnostic accuracy besides its half-life of 6 h which is perfect for diagnostic use with the lowest patient radiation burden. [11]. An important practical advantage of [^{99m}Tc] is its availability through a molybdenum-99/technetium-99m generator system, which allows on-site production in most clinical settings without requiring a cyclotron. Furthermore, [99mTc] exhibits highly versatile chemistry, enabling it to be complexed with a wide range of biologically active molecules to target specific tumor types or

DOI: 10.21608/EPJ.2025.377496.1089

physiological processes (e.g., 99mc-sestamibi for breast cancer or ^{99m}Tc-HMPAO for brain perfusion imaging). This adaptability enhances its clinical utility across multiple oncologic applications[12]. Vanillin derivatives are good biologically active compounds that can be coupled with radioisotopes. It is a specialized metabolite extracted from vanilla beans [13]. It contains several functional groups, including 4-hydroxyl, 3-methoxy, which facilitate their coupling to radioisotopes. It exhibits a range of pharmacological properties, such as anticancer, neuro protective, and antibacterial activities [14-16]. Due to its anti-mutagenic potential, it has been evaluated as an anticancer agent at the molecular level. At a concentration of 1000 µg.mL-1, it inhibits the proliferation of HT-29 colon cancer cells and promotes apoptosis [17]. Furthermore, one of its derivatives, 4-(1H-imidazo[4,5-f][1,10]phenanthrolin-2-yl)-2-methoxyphenol enhances inhibition of invasion and migration in HT-29 and HCT116 cells by targeting the Wnt/βcatenin signaling pathway [18]. This compound also down regulates proteasome genes, the MAPK and NF-κB activity[16]. Another pathway, derivative, VND3207, demonstrates strong radioprotective effects in radiation-induced intestinal injury in mice In vitro studies suggest that this compound can induce apoptosis in human hepatic carcinoma and neuroblastoma cells [19]. Molecular docking has shown high binding affinity to the CAMKIV enzyme in cancer cells[20]. These findings support its potential as an effective carrier for the [99mTc] isotope in targeted tumor imaging. Gallic acid (GA) is a polyphenol compound with the chemical name 3,4,5-trihydroxybenzoic acid and the molecular formula C₇H₆O₅ [21]. Gallic acid derivatives are phytochemicals known to have anticancer activity. GA plays a significant role in suppressing cancer cell proliferation and metastasis by inducing apoptosis (programmed cell death), inhibiting cell proliferation, and suppressing angiogenesis. GA targets cell cycle regulators, apoptosis pathways, and growth factor signaling [22-24]. Cancer management and treatment remain major challenges for researchers in both developed and developing countries. Successful treatment requires early diagnosis, detailed planning, and accurate therapeutic regimens. Even though the number of cancer survivors has increased in the U.S., cancer mortality and morbidity rates remain However, cancer-related deaths decreased due to lifestyle changes, including reduced smoking, increased patient awareness, and early diagnosis [25,26] GA and vanillin exhibit strong affinities for various targets on cancer cells, making them promising carriers for the [99mTc] isotope. They may deliver the isotope to tumors with high specificity while minimizing effects on

normal cells, thus reducing side effects and improving safety [27] In this study, we synthesized a gallic acid derivative (compound 4) and a vanillin derivative (compound 6), which were used as carriers for [99mTc]. Finally, we injected [99mTc] Tc-4 and [99mTc] Tc-6 into tumor-induced mice to evaluate their tumor-to-nontumor (T/NT) ratio using a reference value of 1.5, and expressed the results as a function of percentage control.

Experimental

Materials

Gallic acid (3,4,5-trihydroxybenzoic acid, C₇H₆O₅, MW 170.12 g·mol⁻¹) was purchased from Alphachem. Vanillin (4-hydroxy-3methoxybenzaldehyde, $C_8H_8O_3$, MW 152.15 g·mol⁻¹), ethanol (ethyl alcohol, C₂H₆O, MW 46.07 $g \cdot \text{mol}^{-1}$), trimethoxybenzaldehyde (3,4,5trimethoxybenzaldehyde, C₁₀H₁₂O₄, MW 196.20 g·mol⁻¹), (hydrazinium hydrazine hydrate hydroxide, $N_2H_4\cdot H_2O$, MW 50.06 g·mol⁻¹), acetone (propan-2-one, MW C_3H_6O , g·mol⁻¹), and ammonium hydroxide (aqueous ammonia, NH₄OH, MW 35.05 g·mol⁻¹) were obtained from Sigma-Aldrich and used without further purification. Thin-layer chromatography (TLC) plates were purchased from Merck and used to monitor the progress of reactions. Spots were visualized under a UV lamp at 254 nm. Paper chromatography was carried out using Whatman No.1 filter paper. Infrared (IR) spectra were recorded using a PerkinElmer spectrophotometer (version 10.6.2)at Helwan University. Molecular mass was recorded on LC-MS ES+ and ¹H NMR spectra were recorded on a Bruker spectrometer operating at 400.15 MHz using a 5 mm PABBO BB/ probe head. The measurements were carried out at 300 K with DMSO-d₆ as the solvent at the Faculty of Pharmacy, Ain Shams University (ASU), Cairo, Egypt. Melting points were measured using a Stuart melting point apparatus and are reported uncorrected. Technetium-99m [99mTc] was eluted from a 99Mo/99mTc generator provided by the Egyptian Atomic Energy Authority. Radioactivity measurements performed using a NaI (Tl) gamma-ray scintillation counter (Scaler Ratemeter SR7 130 model, England). Albino mice weighing 20-25 g were used for tumor-targeting studies. Ehrlich ascites carcinoma (EAC) cells were obtained from the National Cancer Institute, Cairo, Egypt. All animals maintained under standard laboratory conditions with free access to food and water. Experimental protocols were approved accordance with institutional ethical guidelines.

Synthesis of (E)-3,4,5-trihydroxy-N'-(3,4,5 trimethoxybenzylidene)benzohydrazide (4)

Gallic acid (1) (1000 mg, 0.0058mmol) was dissolved in 30 ml ethanol and 0.5 ml of Conc. H₂SO₄ was added and then the mixture was refluxed with stirring for 10 hours at 120°C and monitored by TLC to confirm reaction completion. The reaction mixture was neutralized by ammonia, washed with water, and extracted with ethyl acetate three times. The organic layer dried with sodium sulfate and evaporated to afford white crystals of the final product 2 with a yield of 800 mg (68%), m.p 160°C. All spectroscopic and analytical properties were identical to those reported in the literature [28].

Ethyl Gallate 2 (800 mg, 0.004mmol) was dissolved in 30 ml ethanol and hydrazine hydrate (0.512ml, 0.016mmol) was added. Then The mixture was refluxed for 18 hour at 120°C and monitored with TLC until completion. A buffcolored precipitate of product 3 was formed during the reaction, reaching a specific amount beyond which no further precipitation occurred in the reaction mixture. The precipitate was then filtered out, and the reaction mixture was refluxed again under the same conditions with stirring. Notably, a buff-colored precipitate formed once more, repeat this technique to get the all amount of product with a yield of 500 mg (68%) and m.p 295-300 °C. All spectroscopic and analytical properties were identical to those reported in the literature [28]

A mixture of galloyl hydrazide 3 (500 mg, 0.0027mmol) and 3,4,5 tri methoxy benzaldehyde (784 mg, 0.004mmol) was dissolved in 20 ml DMSO then followed by 5 drops of glacial acetic acid. The reaction mixture was refluxed with stirring for 12 hour at 120°C and the reaction was monitored by TLC. The reaction mixture cooled, worked up by adding water and filtrate the precipitate to afford the final product 4, with a yield of 700 mg (71.5 %,) in the form fine brown powder, m.p 300 °C. H NMR spectroscopy (400 MHz, DMSO-d₆) δ 3.71 (s, 3H), 3.76 (s, 3H), 3.84 (s, 3H), 7.10 (s, 1H), 7.25 (s, 1H), 8.09 (s, 1H), 8.32 (s, 1H), 8.65 (s, 1H), 8.74 (s, 1H), 8.85 (s, 1H), 9.24 (s, 1H), and 9.88 (s, 1H). IR Characteristic peaks (OH, 3226) (CH aliphatic ,2941) (C=O , 1667) (C=C , 1577 - 1452). All spectroscopic and analytical properties were identical to those reported in the literature [28]

Synthesis of 4,4'-((1E,1'E)-hydrazine-1,2-diylidenebis(methaneylylidene))bis(2methoxyph enol) (6)

To the solution of vanillin (5) (1gm, 0.0065 mmol) in 20 ml ethanol a hydrazine hydrate (0.5 ml, 0.016 mmol) was added. The reaction mixture was refluxed for 2 hours at 100°C. The reaction mixture was cooled, worked up by adding water and filtering the precipitate to afford the final product 6,

with a yield of 680 mg (70%,) in the form of fine yellow powder, m.p 180°C. LC-MS Characteristic peak at 301 m/z for molecular ion peak , IR Characteristic peaks (OH , 3478) (CH aliphatic ,2919) (C=N , 1624) (C=C , 1450 – 1464). All spectroscopic and analytical properties were identical to those reported in the literature [29]

Radiosynthesis of [99mTc] Tc-4 and [99mTc] Tc-6

[99mTc] Tc-4 and [99mTc] Tc-6 complexes were synthesized using a direct radiolabeling technique. In this method, sodium borohydride is a reducing agent with the chemical formula NaBH₄ was used to reduce technetium-99m in the +7 oxidation state (99mTc(VII)) to a lower oxidation state suitable for complexation with **4** and **6**. The radiolabeling conditions were optimized by investigating the influence of various parameters on the radiochemical yield, including substrate amount, reducing agent amount, pH of the reaction medium, and reaction time

For the labeling procedure, 0.400 mL of an aqueous solution containing 10–300 µg.mL⁻¹ of the substrate was transferred into an evacuated penicillin vial. To this, 0.100 mL of freshly prepared sodium borohydride solution (containing $3-40 \text{ mg.mL}^{-1} \text{ NaBH}_4$) was added. The pH of the reaction mixture was adjusted within the range of 3 to 10 using 0.400 mL of phosphate buffer solution. Then, 0.100 mL of freshly eluted ^{9 9 m} TcO₄ solution (195 MBq) was introduced into the reaction vial. The mixture was incubated at room temperature for various time intervals to determine optimal reaction duration. Following incubation, the in vitro stability of the radiolabeled complexes was evaluated under the optimized conditions

Radiochemical yield evaluation of [99mTc] Tc-4 and [99mTc] Tc-6

The radiochemical yields and in vitro stability of [99mTc] Tc-4 and [99mTc] Tc-6 complexes were determined using ascending paper chromatography (PC).

PC analysis

The radiochemical yield and in vitro stability of the [99mTc] Tc-4 and [99mTc] Tc-6 complexes were evaluated using ascending paper chromatography (P.C.) to determine the percentages of [99mTc] Tc-4, [99mTc] Tc-6 free 99mTcO₄, and reduced hydrolyzed ^{99m}Tc colloid species as follows [30–32]. Each labeling experiment involved ascending chromatography utilizing two strips of Whatman No. 1 paper, (measuring 13 cm in length and 1 cm in width). Two drops of the reaction product were spotted on the line (origin) at a distance of 2 cm from the bottom. One strip was developed using acetone, while the other was developed with a mixture of ethanol, water, and ammonium hydroxide in a 2:5:1 volume ratio (v/v/v). Upon completion of development, the two strips were dried, sectioned into 1 cm segments, and individually quantified utilizing the NaI(Tl) gamma-ray scintillation counter to ascertain the ratios of hydrolyzed ^{99m}Tc, free ^{99m}TcO₄, and the [^{99m}Tc] Tc-4 and [^{99m}Tc] Tc-6 complexes. Every experiment was conducted thrice.

Targeting evaluation of [99mTc] Tc-4 and [99mTc] Tc-6 in tumor bearing mice

Experiments were performed using the procedure that was approved by the animal ethics committee and was in accordance with the guidelines set out by the Egyptian Atomic Energy Authority (No: P/28A/25).

Solid tumor bearing mice

The parent tumor line (Ehrlich ascites carcinoma) was used to induce sarcoma in the left thigh of mice to induce tumor bearing mice models.

Biodistribution assay

A 0.1 ml [99mTc] Tc-4 and [99mTc] Tc-6 complexes (185–1850 KBq) were injected intravenously into the tail vein of solid tumor bearing albino mice of body mass 20–25 g. The animals were weighed, anaesthetized by chloroform and scarified at different time points (15, 30, 60, and 180 min post injection). Organs and tissues were collected, rinsed with saline.

The radioactivity of each sample as well as the back ground was counted in a well-type c-counter NaI(Tl). The percentages of injected doses per gram tissue or organ (% ID/g) in a population of five mice for each time point were calculated for each sample. Solid tumor to normal muscle (T/NT) was calculated from % ID/g for solid tumor and normal muscle [33–35].

Results and discussion Chemistry

Imines are organic compounds containing a carbonnitrogen double bond (C=N), typically formed by the condensation of primary amines with aldehydes by eliminating water. They play a crucial role in pharmaceutical drugs.[36,37]

The synthesis pathway to obtain the title compound (4) is shown in scheme 1. Ethyl gallate (2) was prepared by condensation of gallic acid (1) with ethanol in the presence of H2SO4 as a catalyst. Subsequently, the ethyl gallate (2) and hydrazine hydrate were refluxed in ethanol to obtain the key intermediate galloyl hydrazide (3).

Finally, the intermediate galloyl hydrazide (3) was reacted with commercial 3,4,5 tri methoxy benzaldehyde containing different substitutes to produce the title compound (4) scheme 1. The structure of compound (4) was confirmed by Melting point, IR and 1H NMR as in the literature [28,38]

Scheme1 Synthetic scheme of (E)-3,4,5-trihydroxy-N'-(3,4,5-trimethoxybenzylidene) benzohydrazide (4).

The Schiff's base reaction is a condensation reaction between a primary amine and an aldehyde or ketone, leading to the formation of an imine (Schiff base) with the elimination of water. Schiff bases have widespread applications in biochemistry, coordination chemistry, and

pharmaceuticals as Schiff bases exhibit antibacterial, antifungal, and anticancer properties.[39,40]

The synthesis pathway to obtain the title compound (6) is shown in Scheme 2. Compound (6) was prepared by schiff's base reaction between

compound (5) and hydrazine hydrate using glacial acetic acid as a catalyst. Subsequently, the compound (5) and hydrazine hydrate were refluxed in ethanol to obtain compound (6) (**Scheme 2**).

The structure of compound (6) was confirmed by Melting point, IR , LC-MS and X-ray Crystallographic in the literature [29]

Scheme 2 Synthetic scheme of 4,4'-((1E,1'E)-hydrazine-1,2-diylidenebis(methaneylylidene))bis(2-methoxyphenol) (6)

X-ray Crystallographic Analysis of 6 [41]

The molecular structure of **6** was determined using X-ray crystallography, providing precise atomic connectivity and spatial orientation. The crystallographic data confirm the expected molecular framework, with well-defined bond lengths and angles. The structure reveals the presence of key functional groups, including hydroxyl (-OH), carbonyl (C=O), and nitrogen containing linkages, which contribute to the compound's chemical stability and potential biological activity.

As shown in **Figure 1**, oxygen atoms are depicted in red, nitrogen in blue, carbon in gray, and hydrogen in white. The molecular arrangement indicates the presence of strong intramolecular interactions, which may enhance the compound's stability and reactivity. These findings are crucial for understanding the physicochemical properties of **6**.

Fig. 1 X-ray crystallographic structure of 6

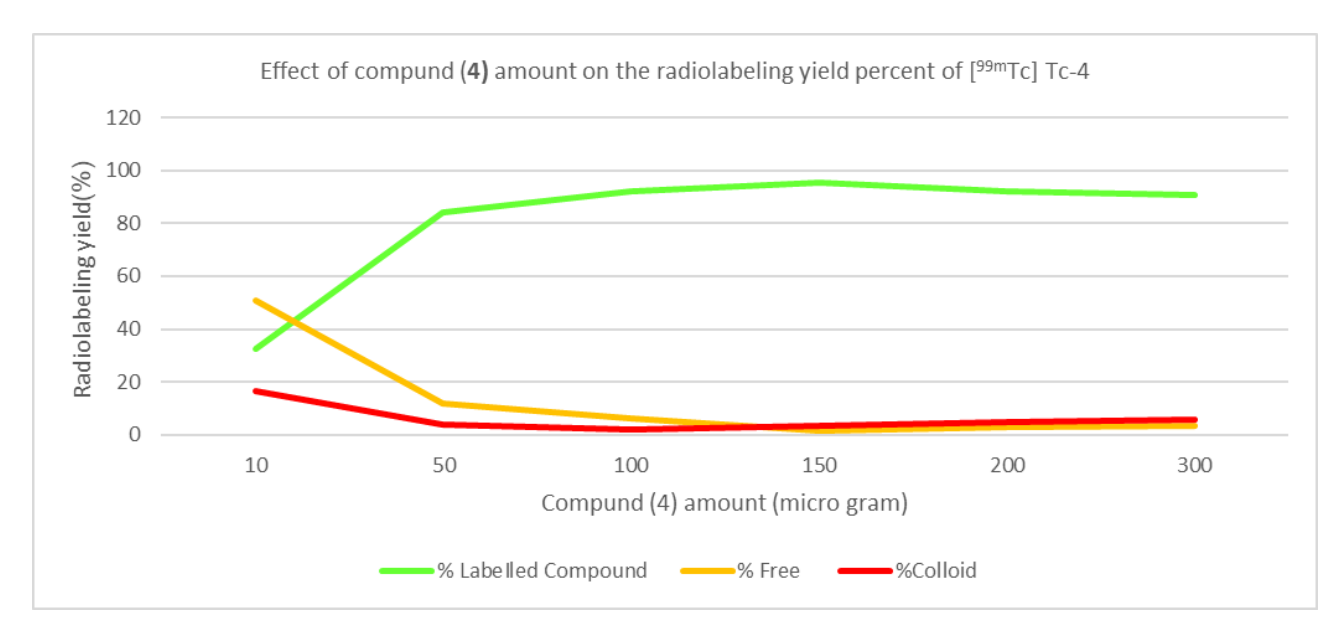


Fig. 2 Effect of compound 4 amount on the radiolabeling yield percent of [99m Tc] Tc-4. Data were presented as mean \pm SD (n = 3).

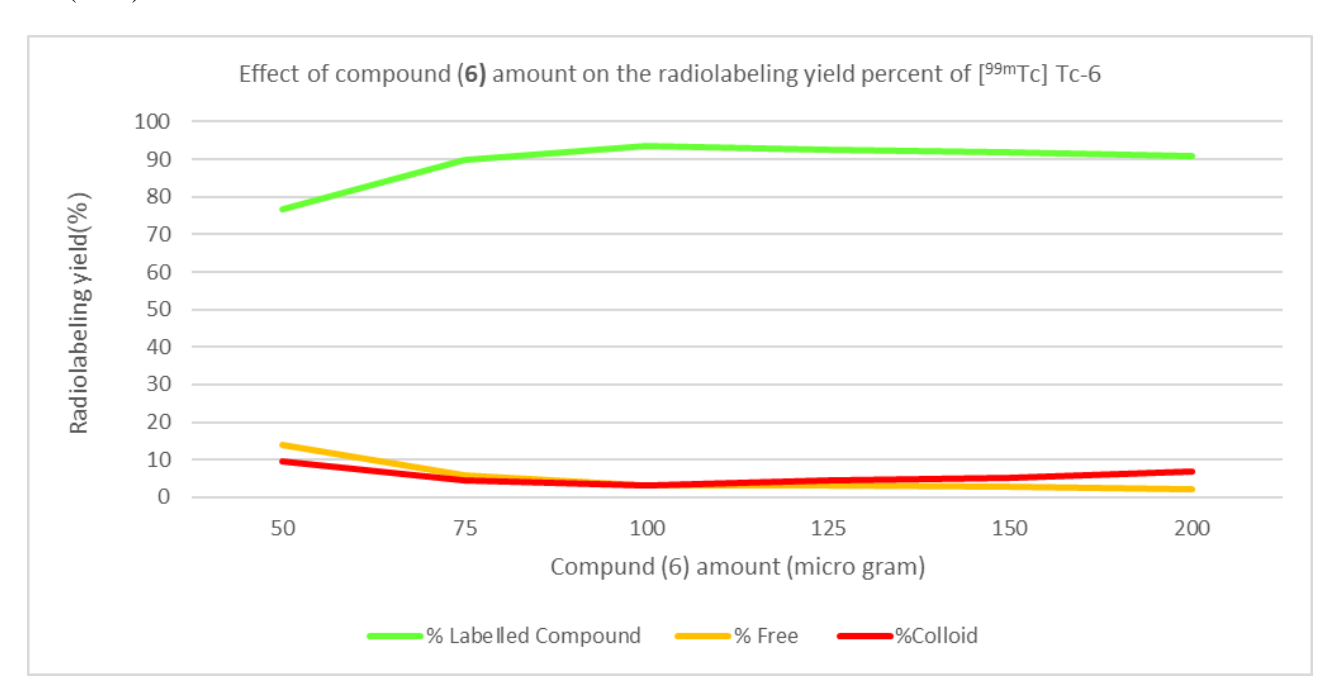


Fig. 3 Effect of compound 6 amount on the radiolabeling yield percent of [99m Tc] Tc-6. Data were presented as mean \pm SD (n = 3).

Factors affecting Radiolabeling yield % of $[^{99m}Tc]\ Tc\text{-}4$ and $[^{99m}Tc]\ Tc\text{-}6$

Radiochemical yield is calculated as follows: Acetone served as the developing solvent for one paper strip, where free 99m TcO₄ migrated with the solvent front (R_f= 1), whereas [99mTc] Tc-4, [99mTc] Tc-6, and reduced hydrolyzed technetium colloid remained at the origin. A solvent composed of ethanol, water, and ammonium hydroxide in a ratio of 2:5:1 (v/v/v) was used for developing an paper additional strip, where reduced hydrolyzed technetium colloid remained at the origin ($R_f = 0$), but free $^{99m}TcO_4$, $[^{99m}Tc]$ Tc-4 and [99mTc] Tc-6 species migrated with the solvent front $(R_f = 1)$. The labeling yield

percentage of the [^{99m}Tc] Tc-4 and [^{99m}Tc] Tc-6 complexes was determined as follows:

% Radiochemical yield = 100 - (% Free 99m TcO $_4$ + % Colloid) (Eq. 1)[42].

Effect of (4) and (6) amounts on radiochemical vield

4 and **6** contents affect the radiochemical yields' percent. The highest radiochemical yield of **4** was 95.3% at 150 microgram, While 93.6% at 100 microgram for **6**. The lower amounts of the **4** and **6**, he lower radiochemical yield because of insufficient substrate amount to chelate all the reduced $[^{99m}Tc]$ species; also, by increasing **4** and **6** amount the radiochemical yield declined.

Effect of Reducing agent of the reaction mixture for 4 and 6

NaBH₄ was used for the reduction of pertechnetate from higher oxidation state (+7) to a lower oxidation state. The maximum radiochemical yield of **4** was 95.3% at 15 mg of NaBH₄, while 93.6% at 10 mg of NaBH₄ for **6**. At lower NaBH₄ content, the radiochemical yield of ^{99m}Tc -4 and ^{99m}Tc -6 was decreased due to the incomplete reduction of $^{99m}TcO_4^-$; also, at higher contents of NaBH4, the radiochemical yield decreased, while the reduced hydrolyzed technetium (RH- $^{99m}_{Tc}$) formation increased.

Effect of the pH of the reaction medium

The pH of the reaction medium significantly influences the radiochemical yield of the 99mTclabeled complexes. For [99mTc] Tc-4, the highest radiochemical yield (95.3%) was obtained at pH 8, whereas for [99mTc] Tc-6, the optimal yield (93.6%) was achieved at pH 9. At lower pH values, the percentage of free pertechnetate (99mTcO₄⁻) increased, leading to a decrease in radiochemical yield. Conversely, at higher pH levels, radiochemical yield was negatively affected due to the increased formation of 99mTccolloid (RH–^{99m}Tc), which represents the primary radiochemical impurity. Therefore, maintaining the reaction pH within the optimal range is critical to minimizing impurities and maximizing labeling efficiency.

Effect of the pH of the reaction medium

The pH of the reaction medium significantly influences the radiochemical yield of the 99mTclabeled complexes. For [99mTc] Tc-4, the highest radiochemical yield (95.3%) was obtained at pH 8, whereas for [99mTc] Tc-6, the optimal yield (93.6%) was achieved at pH 9. At lower pH values, the percentage of free pertechnetate (99mTcO₄⁻) increased, leading to a decrease in radiochemical yield. Conversely, at higher pH levels, radiochemical yield was negatively affected due to the increased formation of 99mTccolloid (RH-^{99m}Tc), which represents the primary radiochemical impurity. Therefore, maintaining the reaction pH within the optimal range is critical to minimizing impurities and maximizing labeling efficiency.

Effect of reaction time on the radiolabeling yield percent of [99mTc] Tc-4 and [99mTc] Tc-6 Optimizing reaction time is a key factor in enhancing radiolabeling purity and understanding the kinetic behavior of the labeling process exergonic reactions, known for their spontaneity and thermodynamic favorability, typically proceed rapidly.

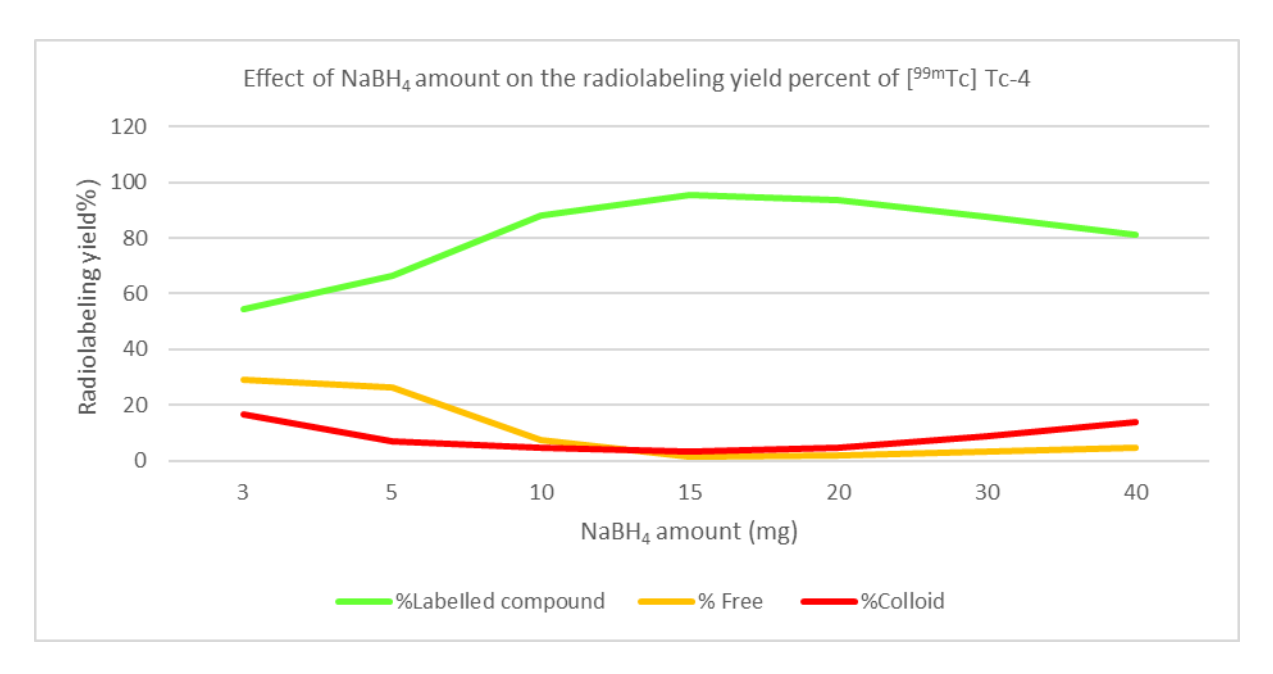


Fig. 4. Effect of NaBH4 amount on the radiolabeling yield percent of [99 mTc] Tc-4. Data were presented as mean \pm SD (n = 3)

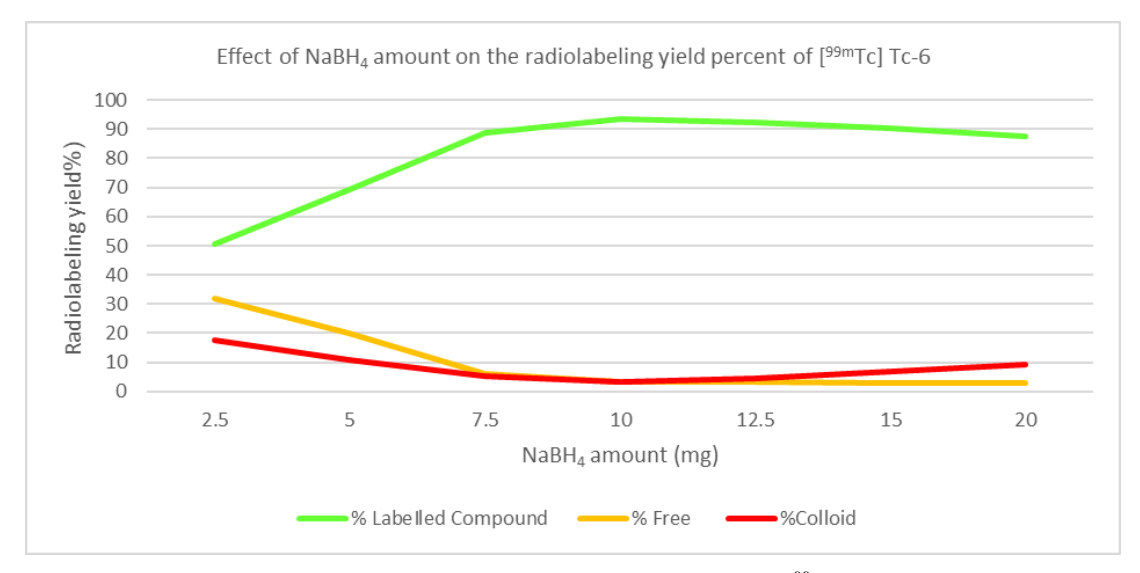


Fig. 5. Effect of NaBH4 amount on the radiolabeling yield percent of [99m Tc] Tc-6. Data were presented as mean \pm SD (n = 3).

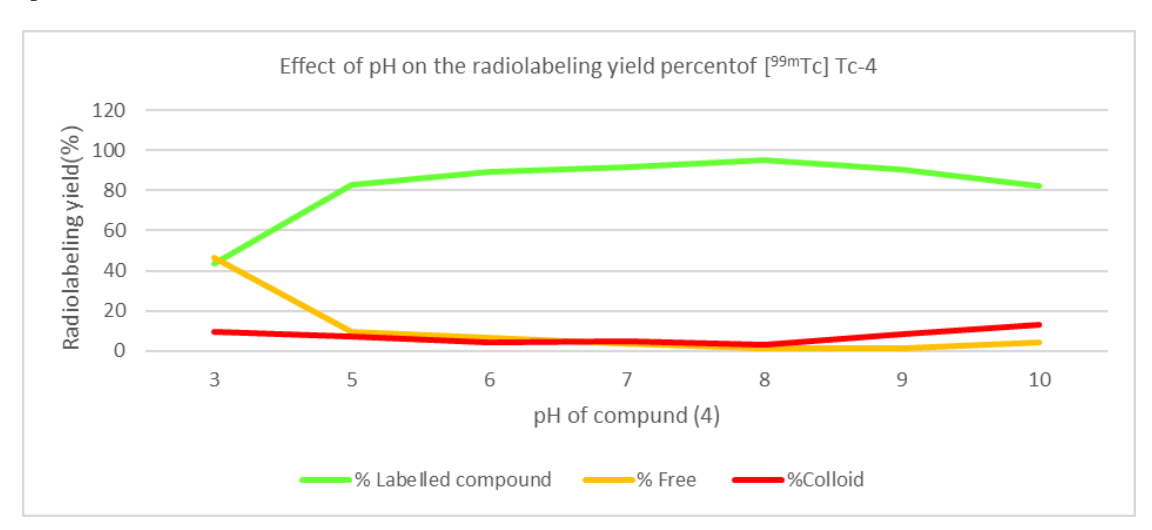


Fig. 6. Effect of pH on the radiolabeling yield percent of [99m Tc] Tc-4. Data were presented as mean \pm SD (n = 3).

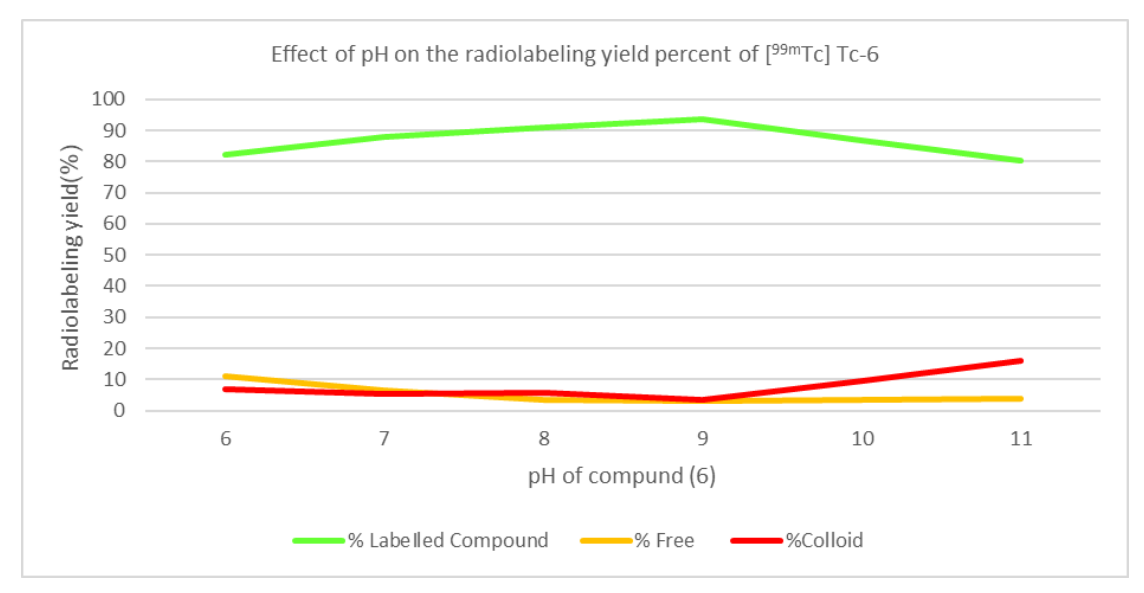


Fig. 7 Effect of pH on the radiolabeling yield percent of [99m Tc] Tc-6, Data were presented as mean \pm SD (n = 3).

As shown in **Figure 8**, [99mTc] Tc-4 achieved its highest radiolabeling yield within the 5–30 minute range, indicating a rapid complexation rate. The labeled complex remained stable for over 12 hours, suggesting a favorable thermodynamic profile characterized by a negative Gibbs free energy change (ΔG). This negative ΔG likely results from a decrease in system enthalpy coupled with an increase in entropy. However, a slight decrease in radiochemical yield was observed at the 60-minute mark. This reduction may be attributed to prolonged exposure to the reducing agent sodium borohydride (NaBH₄), or to the formation of oxidative colloidal byproducts due to radiolysis. Such factors can chelation negatively affect stability

compromise the structural integrity of the labeled complex over time.

Similarly, as shown in **Figure 9**, the optimal labeling yield for [^{99m}Tc] Tc-6 was also observed within the 5–30 minute interval. The formulation demonstrated efficient and rapid complexation, suggesting favorable reaction kinetics. The thermodynamic profile, again, indicates a likely decrease in Gibbs free energy (ΔG), reflecting increased entropy and reduced enthalpy during the chelation process. Beyond 30 minutes, a minor reduction in labeling yield was noted, possibly due to extended exposure to NaBH₄. Prolonged reaction times can promote unwanted redox side reactions or radiolytic degradation, thereby disrupting the chelation efficiency and structural stability of the labeled compound.

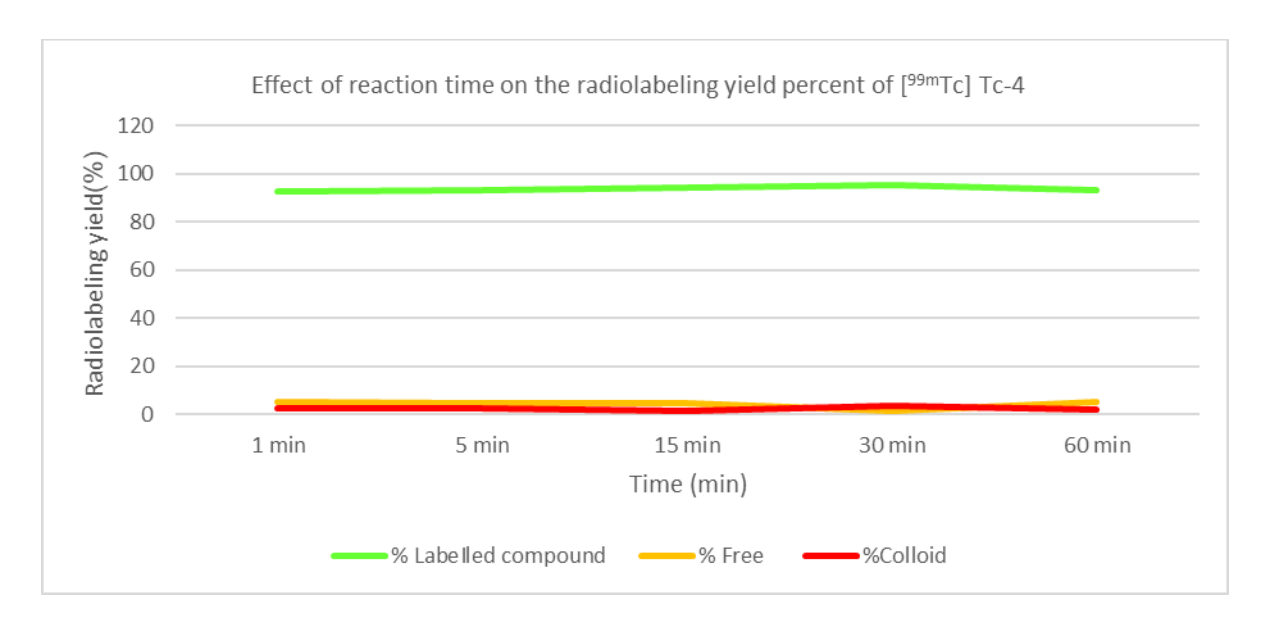


Fig. 8 Effect of reaction time on the radiolabeling yield percent of [99m Tc] Tc-4. Data were presented as mean \pm SD (n = 3).

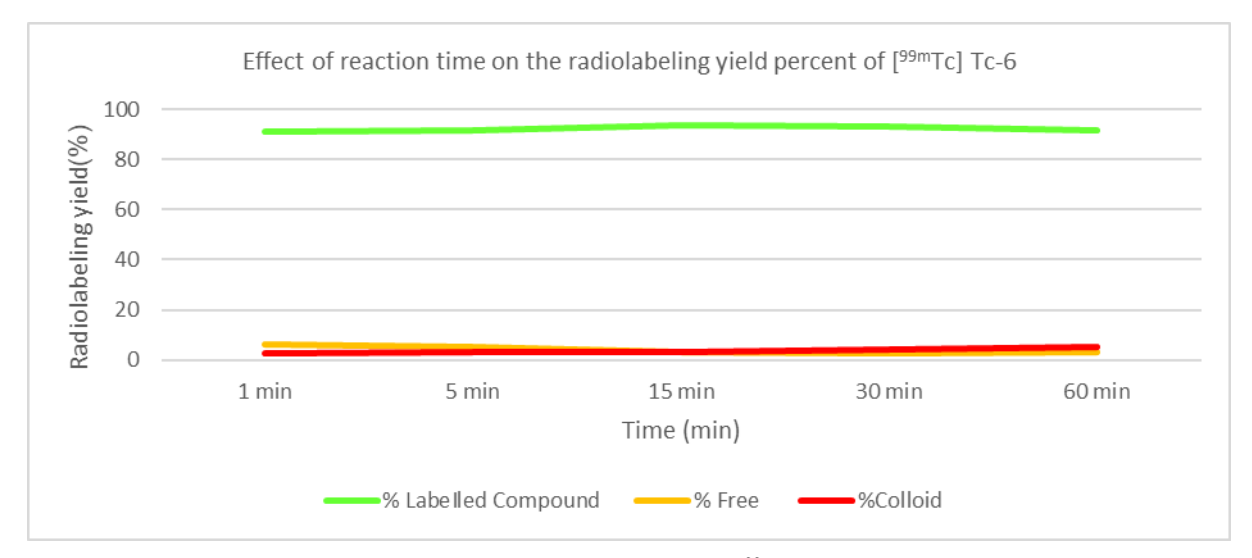


Fig. 9 Effect of reaction time on the radiolabeling yield percent of [99m Tc] Tc-6. Data were presented as mean \pm SD (n = 3).

Effect of in vitro stability on the radiolabeling yield percent of [99mTc] Tc-4 and [99mTc] Tc-6

he in vitro stability assessment was conducted to evaluate the durability of the radiolabeled formulations during pharmaceutical handling and their suitability for clinical application in hospital settings [33,43,44] **Figure 10** illustrates the stability profile of [^{99m}Tc] Tc-4, showing a consistently high radiolabeling yield sustained over 24 hours. The complex demonstrated excellent stability in physiological 0.9% saline, with radiolabeling yields exceeding 85%. This result highlights the strong coordination between ^{99m}Tc and the ligand matrix **4**, providing sufficient time stability for hospital compounding and short-term storage.

Similarly, **Figure 11** shows the stability profile of [^{99m}Tc] Tc-6. The formulation retained over 84% radiochemical purity after 24 hours in 0.9% saline, indicating a satisfactory shelf-life. This consistent in vitro stability suggests strong binding affinity between technetium and the functional groups in compound 6, making it a promising candidate for clinical radiopharmacy use.

Targeting evaluation of [99mTc] Tc-4 and [99mTc] Tc-6 in tumor bearing mice

The bio-distribution of [99mTc]Tc-4 and [99mTc]Tc-6 in solid tumor-bearing mice was evaluated at 15, 30, 60, and 180 minutes post-injection, with radioactivity levels expressed as the percent of

injected dose per gram (% ID/g ± SEM) for five mice per group. The primary parameter used to assess their tumor selectivity was the target-tonontarget (T/NT) ratio between the tumor tissue and normal muscle tissue The T/NT ratio of radiopharmaceuticals represents their capability to target specific tumor receptor and literatures stated that T/NT ratio greater than 1.5 proves the potentiality of these radiopharmaceuticals diagnostic agents [45,46]. The results revealed that [99mTc] Tc-4 exhibited a T/NT ratio of 1.3 at 15 minutes, which gradually increased to its highest value of 1.74 at 60 minutes post-injection, indicating modest tumor selectivity. In contrast, [99mTc]Tc-6 showed a T/NT ratio of 1.49 at 15 minutes, which markedly rose to 4.32 at 60 reflecting strong tumor minutes. capability. These findings were compared to the previously reported [99mTc]Ifosfamide complex, which demonstrated a T/NT ratio of 2.9 at 60 min under similar experimental conditions [47]. Based on these results, [99mTc] Tc-6 exhibited superior tumor selectivity compared to both [99mTc]Ifosfamide [^{99m}Tc]Tc-4. and while [99mTc]Tc-4 achieved acceptable but moderate targeting efficiency. These results emphasize the promising potential of [99mTc]Tc-4 and [99mTc] Tc-6 as an effective radiopharmaceutical candidate for tumor imaging applications.

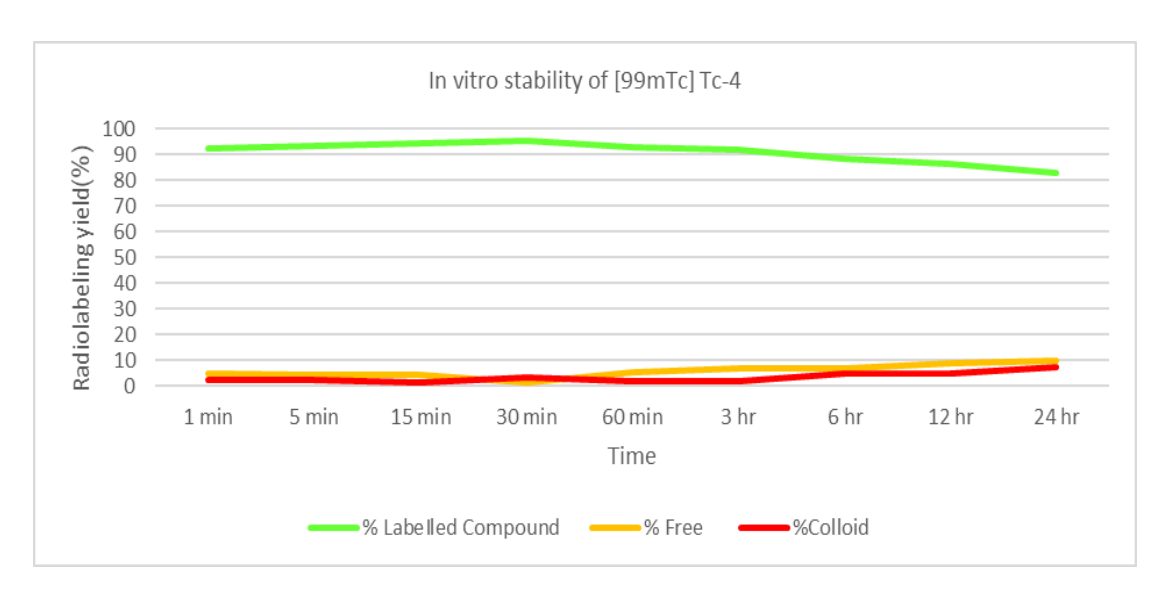


Fig. 10 Effect of in-vitro stability on the radiolabeling yield percent of [99m Tc] Tc-4. Data were presented as mean \pm SD (n = 3).



Fig. 11 Effect of in-vitro stability on the radiolabeling yield percent of $[^{99m}Tc]$ Tc-6. Data were presented as mean \pm SD (n = 3).

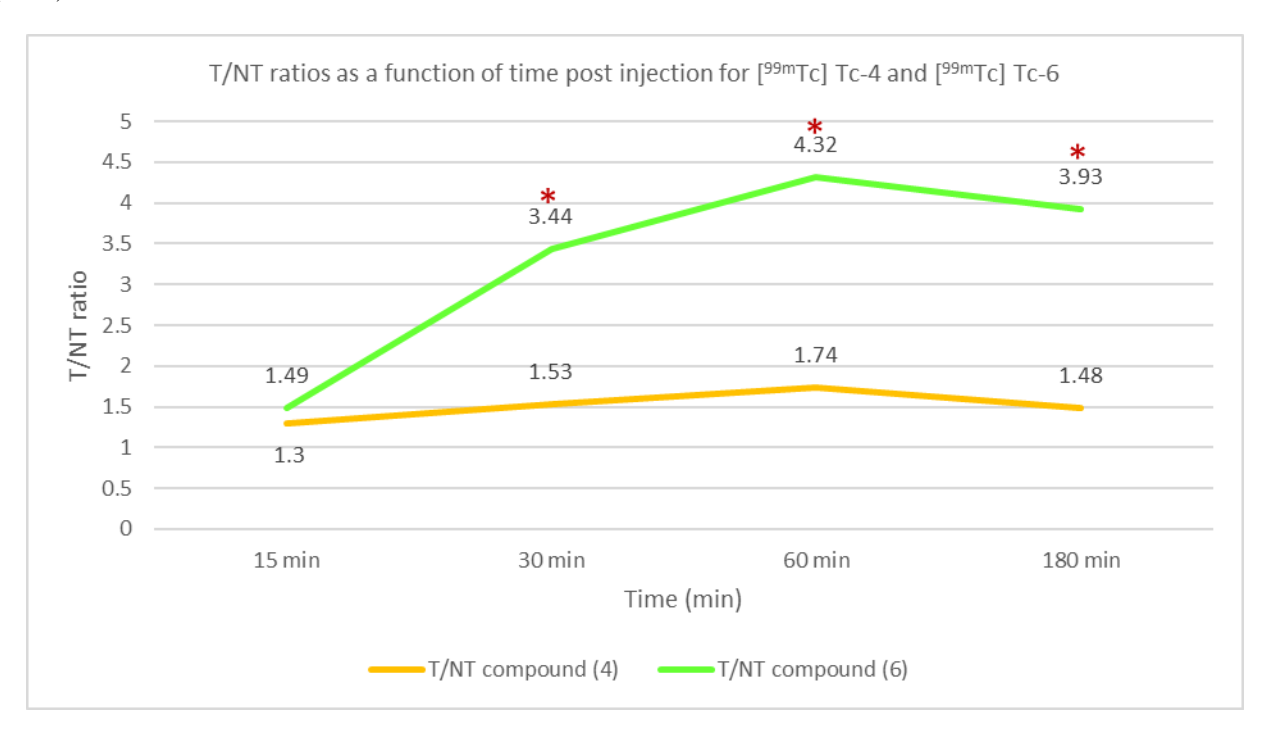


Fig. 12. T/NT ratios as a function of time post injection for $[^{99m}Tc]$ Tc-4 and $[^{99m}Tc]$ Tc-6. Data were presented as mean \pm SD (n = 3). * Significant difference compared to reference standard. Note: The reference standard refers to the universal threshold value (T/NT = 1.5) commonly used in the literature to indicate effective tumor-targeting capability.

In Vivo Biodistribution of [99mTc] Tc-4 in Tumor-Bearing Mice

The biodistribution of [99mTc] Tc-4 which, is developed as a tumor-targeting imaging agent, was timely evaluated to monitor its biolocalization in various tissues for better understanding their pharmacokinetic (ADME: Absorption, distribution, metabolism and excretion) analysis. The study was performed at 0.25, 0.5, 1, and 3 hours postinjection, with results expressed as % administered dose per gram /tissue (ID/g). Fig. 13, illustrates the

biolocalization in Ehrlich tumor-bearing mice which demonstrated marked tumor uptake, highlighting the tumor-affinity of [99mTc] Tc-4 at 15 minutes post intravenous injection, blood, liver, kidneys, and intestines exhibited prompt radiotracer accumulation, indicating rapid systemic uptake. As the time passes, the uptake in the liver, and intestines progressively increase, which may be attributed to enterohepatic circulation and first-pass metabolism. By the 3-hour time point, significant clearance from the blood was found, while the heart and spleen showed an increase in the radiotracer

selectivity. This may be explained by the formation of monocationic species, behaving like monocationic transport properties of sodium ions. A generalized clearance was observed in most organs, with the exception of the tumor, where uptake which progressively increase over time, indicating tumor-specificity of [99mTc] Tc-4.

Renal excretion increases after 30 minutes, indicating primary excretion via the kidnevs. Gradual increase in gastrointestinal uptake was shown which may be due to possible degradation of [99mTc] Tc-4, leading to the release of free pertechnetate. The thermodynamic of this reaction, characterized by a negative Gibbs free energy (ΔG), which favors the backward radiolysis of [99mTc] Tc-4, particularly at physiological body temperature [9,43,48]. Additionally, the presence of endogenous reducing agents and oxidizing agents, including glutathione, ascorbic acid, and uric acid, may contribute to oxidative byproducts that affect the radiotracer stability and biodistribution. These total findings suggest that [99mTc] Tc-4 exhibits high tumor selectivity, with increasing tumor uptake over time, elucidating its value as a promising tumor-imaging and theranostic candidate.

Bio distribution of [99mTc] Tc-6 in Tumor-Bearing Mice

To evaluate the tumor-targeting of [99mTc] Tc-6, bio distribution studies were performed in Ehrlich tumor-bearing mice at different time intervals: 15 min, 30 min, 1 h, and 3 h post-injection. The radio uptake were calculated as percentage of injected dose per gram of tissue (%ID/g). This data highlights how the compound is absorbed, distributed, metabolized, and elucidated as its ADME profile.

After 15 minutes post-IV injection, significant radioactivity amount was detected in the blood, liver, kidneys, and intestines, suggesting that the

compound rapidly enters systemic circulation. As the time passes, radio uptake in the liver and intestines continued to rise, indicating first-pass metabolism and entero-hepatic circulation. Finally, by the 3-hour, there was a marked decrease in blood radioactivity, confirming effective systemic body clearance. The tumor uptake increases with the time passing of the study, reflecting a selective bio-accumulation in tumor tissue. This could be attributed to enhanced permeability and retention (EPR) effects or possible interaction with tumor-specific receptors. The lower clearance from tumor tissue during the observed the experiments further support the selective retention of the 6 at the target site.

The spleen and heart showed mild increases in radioactivity uptake up to 3 hours, which may be explained by binding due to formation of monocationic species mimicking endogenous ions, like sodium. Renal activity started to rise, pointing toward renal excretion as a key elimination route. Meanwhile, intestinal radioactivity increased, possibly due to partial decomposition of the radiolabelled complex, resulting in free pertechnetate release. This behavior may thermodynamically explained by a negative Gibbs free energy change (ΔG) that favors backward degradation at body temperature. Also the in vivo biochemical environment which is rich in redoxactive molecules like glutathione, uric acid, and ascorbate, could contribute to partial oxidation or reduction of technetium, destabilizing the complex and altering its biodistribution. Taken together, these results suggest that [99mTc] Tc-6 maintains high tumor selectivity, with increasing uptake over time, making it a strong candidate for tumor imaging and theranostic development.

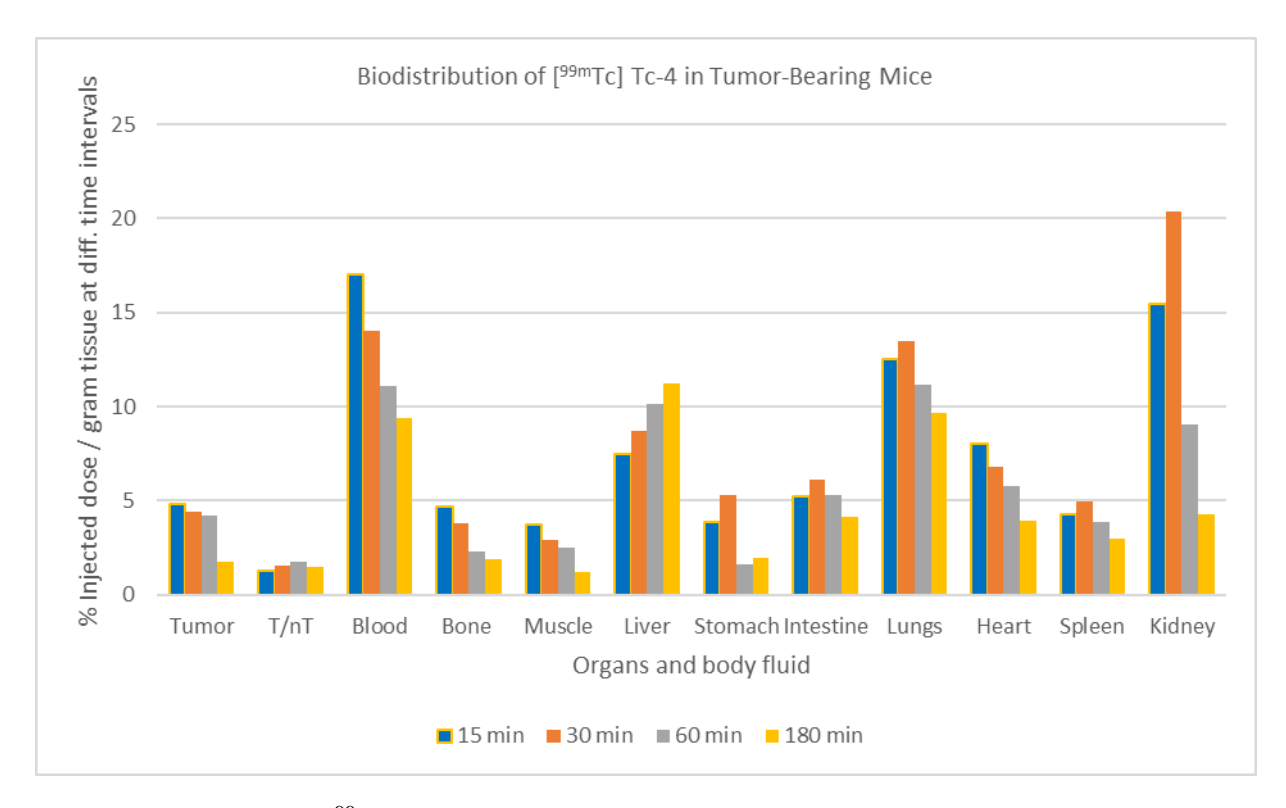


Fig. 13 Biodistribution of [99m Tc] Tc-4 in Tumor-Bearing Mice. Data were presented as mean \pm SD (n = 3).

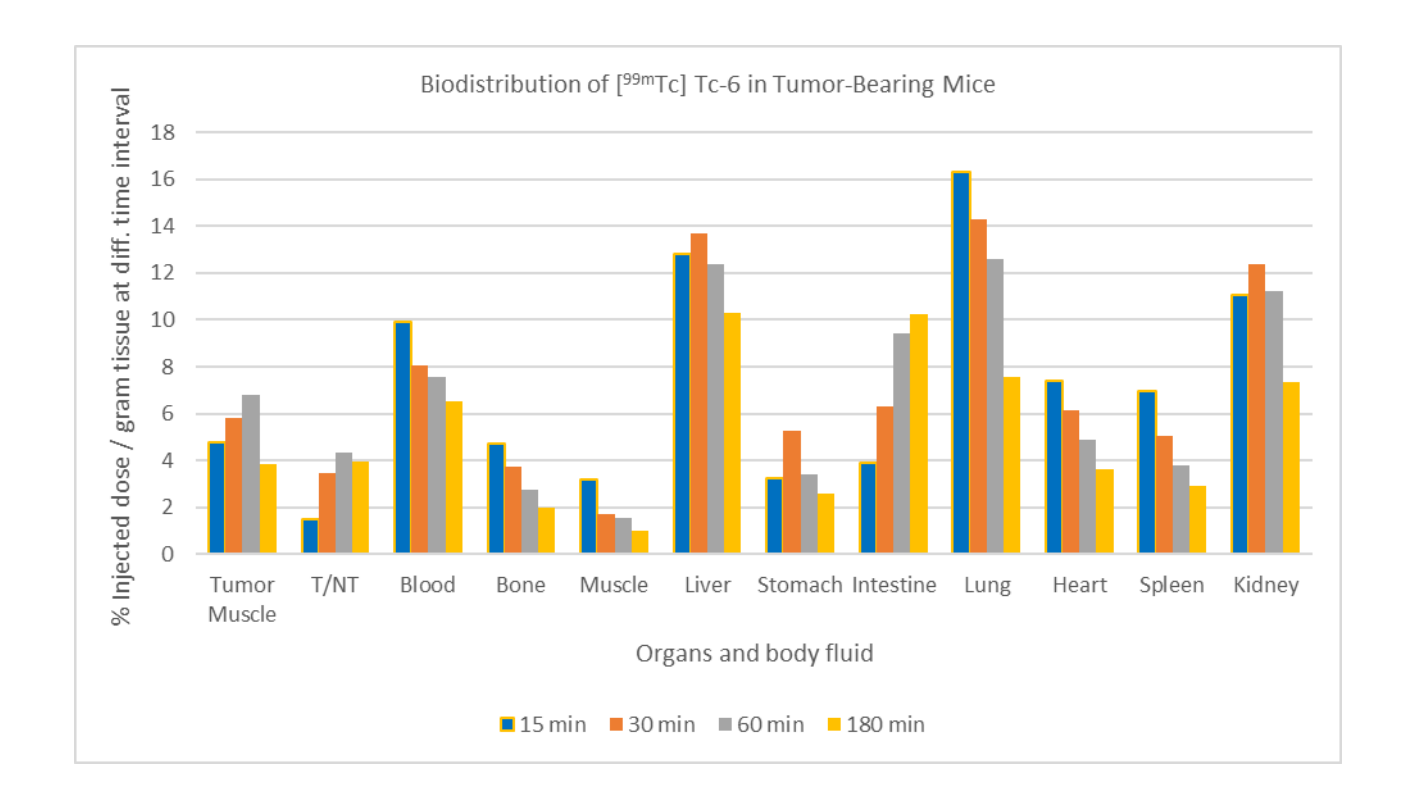


Fig. 14 Biodistribution of [99m Tc] Tc-6 in Tumor-Bearing Mice. Data were presented as mean \pm SD (n = 3).

Conclusion

This study successfully synthesized and evaluated two novel radiopharmaceutical agents, [99mTc] Tc-4 and [99mTc] Tc-6, derived from gallic acid and vanillin respectively, for targeted tumor imaging. Both compounds demonstrated high radiochemical yields under optimized conditions, along with excellent in vitro stability. Biodistribution studies in tumor-bearing mice revealed strong tumor affinity, particularly for [99mTc] Tc-6, which achieved a T/NT ratio of 4.32 at 60 minutes post-injection. results confirm the tumor-targeting efficiency of both agents and highlight their potential as selective carriers for technetium-99m in oncological imaging. Given their promising performance, future studies should explore their application with other isotopes, long-term safety, and imaging efficacy in clinical trials, aiming to establish [99mTc] Tc-4 and [99mTc] Tc-6 as reliable candidates for cancer diagnostics and theranostics.

Conflict of interest

There is no conflict of intersrt

Acknowledgment

Prof. Wafaa A. Zaghary expresses her grateful appreciation and thanks for Research support center, Helwan University, Egypt for funding this work.

References

- Singh SK, Singh S, Lillard Jr JW, Singh R. Drug delivery approaches for breast cancer. Int J Nanomedicine. 2017;6205–18.
- Sung H, Ferlay J, Siegel RL, Laversanne M, Soerjomataram I, Jemal A, et al. Global Cancer Statistics 2020: GLOBOCAN Estimates of Incidence and Mortality Worldwide for 36 Cancers in 185 Countries. CA Cancer J Clin. 2021 May;71(3):209–49.
- Lau KH, Tan AM, Shi Y. New and emerging targeted therapies for advanced breast cancer. Int J Mol Sci. 2022;23(4):2288.
- Abdulwahab HG, Harras MF, El Menofy NG, Hegab AM, Essa BM, Selim AA, et al. Novel thiobarbiturates as potent urease inhibitors with potential antibacterial activity: Design, synthesis, radiolabeling and biodistribution study. Bioorg Med Chem. 2020;28(23):115759.
- Nasr T, Bondock S, Ibrahim TM, Fayad W, Ibrahim AB, AbdelAziz NA, et al. New acrylamide-sulfisoxazole conjugates as dihydropteroate synthase inhibitors. Bioorg Med Chem. 2020 May;28(9):115444.
- Khedr MA, Rashed HM, Farag H, Sakr TM. Rational design of some substituted phenyl azanediyl (bis) methylene phosphonic acid derivatives as potential anticancer agents and imaging probes: Computational inputs, chemical synthesis, radiolabeling, biodistribution and gamma scintigraphy. Bioorg Chem. 2019 Nov;92:103282.

- Nasr T, Bondock S, Rashed HM, Fayad W, Youns M, Sakr TM. Novel hydrazide-hydrazone and amide substituted coumarin derivatives: Synthesis, cytotoxicity screening, microarray, radiolabeling and in vivo pharmacokinetic studies. Eur J Med Chem. 2018;151:723–39.
- Mohamed KO, Nissan YM, El-Malah AA, Ahmed WA, Ibrahim DM, Sakr TM, et al. Design, synthesis and biological evaluation of some novel sulfonamide derivatives as apoptosis inducers. Eur J Med Chem. 2017;135:424–33.
- Al-Wabli RI, Sakr TMMH, Khedr MA, Selim AA, El-Rahman MAEMA, Zaghary WA. Platelet-12 lipoxygenase targeting via a newly synthesized curcumin derivative radiolabeled with technetium-99m. Chem Cent J. 2016;10:1–12.
- Boschi A, Uccelli L, Marvelli L, Cittanti C, Giganti M, Martini P. Technetium-99m Radiopharmaceuticals for Ideal Myocardial Perfusion. Molecules. 2022 Feb;27(4).
- Mushtaq S, Bibi A, Park JE, Jeon J. Recent Progress in Technetium-99m-Labeled Nanoparticles for Molecular Imaging and Cancer Therapy. Vol. 11, Nanomaterials. 2021.
- Cherry SR, Sorenson JA, Phelps ME. Physics in nuclear medicine. Soc Nuclear Med; 2013.
- Zhang S, Mueller C. Comparative analysis of volatiles in traditionally cured Bourbon and Ugandan vanilla bean (Vanilla planifolia) extracts. J Agric Food Chem. 2012;60(42):10433–44.
- 14. Arya SS, Sharma MM, Das RK, Rookes J, Cahill D, Lenka SK. Vanillin mediated green synthesis and application of gold nanoparticles for reversal of antimicrobial resistance in Pseudomonas aeruginosa clinical isolates. Heliyon. 2019;5(7).
- Bezerra DP, Soares AKN, De Sousa DP. Overview of the role of vanillin on redox status and cancer development. Oxid Med Cell Longev. 2016;2016.
- 16. Li JM, Lee YC, Li CC, Lo HY, Chen FY, Chen YS, et al. Vanillin-ameliorated development of azoxymethane/dextran sodium sulfate-induced murine colorectal cancer: the involvement of proteasome/nuclear factor-κB/mitogen-activated protein kinase pathways. J Agric Food Chem. 2018;66(22):5563–73.
- 17. Ramadoss DP, Sivalingam N. Vanillin extracted from Proso and Barnyard millets induce apoptotic cell death in HT-29 human colon cancer cell line. Nutr Cancer. 2020;72(8):1422–37.
- 18. Ma W, Li X, Song P, Zhang Q, Wu Z, Wang J, et al. A vanillin derivative suppresses the growth of HT29 cells through the Wnt/β-catenin signaling pathway. Eur J Pharmacol. 2019;849:43–9.
- Naz H, Tarique M, Khan P, Luqman S, Ahamad S, Islam A, et al. Evidence of vanillin binding to CAMKIV explains the anti-cancer mechanism in human hepatic carcinoma and neuroblastoma cells. Mol Cell Biochem. 2018;438:35– 45.
- Jantaree P, Lirdprapamongkol K, Kaewsri W, Thongsornkleeb C, Choowongkomon K, Atjanasuppat K, et al. Homodimers of vanillin and apocynin decrease the metastatic potential of human cancer cells by inhibiting the FAK/PI3K/Akt signaling pathway. J Agric Food Chem. 2017;65(11):2299–306.
- Dludla P V, Nkambule BB, Jack B, Mkandla Z, Mutize T, Silvestri S, et al. Inflammation and oxidative stress in an obese state and the protective effects of gallic acid. Nutrients. 2018;11(1):23.
- 22. Lu Y, Jiang F, Jiang H, Wu K, Zheng X, Cai Y, et al. Gallic acid suppresses cell viability, proliferation, invasion and angiogenesis in human glioma cells. Eur J Pharmacol. 2010 Sep;641(2–3):102–7.
- Bray F, Ferlay J, Soerjomataram I, Siegel RL, Torre LA, Jemal A. Global cancer statistics 2018: GLOBOCAN

- estimates of incidence and mortality worldwide for 36 cancers in 185 countries. CA Cancer J Clin. 2018;68(6):394–424.
- 24. Cahyana AH, Desta I, Amaliyah L, Nadia A, Sahaya HD, Annas D, et al. Synthesis of Mannich N-bases based on benzimidazole derivatives using SiO2[sbnd]OAlCl2 catalyst and their potential as antioxidant, antibacterial, and anticancer agents. South African J Chem Eng. 2025;51(May 2024):95–111.
- 25. Siegel RL, Miller KD, Fuchs HE, Jemal A. Cancer Statistics, 2021. CA Cancer J Clin. 2021 Jan;71(1):7–33.
- 26. Hussien NA, Khalil MAEF, Schagerl M AS. Green Synthesis of Zinc Oxide Nanoparticles as a Promising Nanomedicine Approach for Anticancer Antibacterial and Anti-Inflammatory Therapies.
- 27. Al-Mudhafar MMJ, Wadi JS. Synthesis and biological activity evaluation of new isatin-gallate hybrids as antioxidant and anticancer agents (in vitro) and in silico study as anticancer agents and coronavirus inhibitors. Pharmacia. 2024;71:1–11.
- 28. Peng Z, Li Y, Tan L, Chen L, Shi Q, Zeng QH, et al. Anti-tyrosinase, antioxidant and antibacterial activities of gallic acid-benzylidenehydrazine hybrids and their application in preservation of fresh-cut apples and shrimps. Food Chem [Internet]. 2022;378(May 2021):132127. Available from: https://doi.org/10.1016/j.foodchem.2022.132127
- 29. Shi J, Zhou Y, Wang K, Ma Q, Wei R, Li Q, et al. Design, synthesis and biological evaluation of Schiff's base derivatives as multifunctional agents for the treatment of Alzheimer's disease. Med Chem Res [Internet]. 2021;30(3):624–34. Available from: http://dx.doi.org/10.1007/s00044-020-02666-6
- 30. Upmanyu N, Garg G, Dolly A, Gupta BN, Mishra P. Triazoles: as promising medicinal agents. Pharmainfo. 2006;4(3).
- Motaleb MA. Preparation and biodistribution of 99m Tclomefloxacin and 99m Tc-ofloxacin complexes. J Radioanal Nucl Chem. 2007;272:95–9.
- 32. Hall A V, Solanki KK, Vinjamuri S, Britton KE, Das SS. Evaluation of the efficacy of 99mTc-Infecton, a novel agent for detecting sites of infection. J Clin Pathol. 1998;51(3):215–9.
- 33. Sakr TM, El- Safoury DM, Awad GAS, Motaleb MA. Biodistribution of 99mTc- sunitinib as a potential radiotracer for tumor hypoxia imaging. J Label Compd Radiopharm. 2013;56(8):392–5.
- Rhodes BA. Considerations in the radiolabeling of albumin. In: Seminars in nuclear medicine. Elsevier; 1974. p. 281–93.
- 35. Ding R, He Y, Xu J, Liu H, Wang X, Feng M, et al. Preparation and bioevaluation of 99m Tc nitrido radiopharmaceuticals with pyrazolo [1, 5-a] pyrimidine as tumor imaging agents. Med Chem Res. 2012;21:523–30.
- 36. de França IV, Döring TH, de Oliveira Neto FM, Pedroso MJ, da Cruz Júnior JW. Imines and their metal complexes as active. J Mol Struct [Internet]. 2024;1314:138725. Available from: https://www.sciencedirect.com/science/article/pii/S002228 6024012444
- Singh GS. Chapter 15 Green chemistry of evergreen imines in the synthesis of nitrogen-containing heterocycles.
 In: Brahmachari GBTGSA for BRH (Second E, editor.

- Advances in Green and Sustainable Chemistry [Internet]. Elsevier; 2021. p. 655–87. Available from: https://www.sciencedirect.com/science/article/pii/B978012 8207925000093
- 38. Rabie AM. Accurate conventional and microwave-assisted synthesis of galloyl hydrazide. MethodsX [Internet]. 2020;7:100737. Available from: https://doi.org/10.1016/j.mex.2019.11.010
- 39. da Silva CM, da Silva DL, Modolo L V, Alves RB, de Resende MA, Martins CVB, et al. Schiff bases: A short review of their antimicrobial activities. J Adv Res [Internet]. 2011;2(1):1–8. Available from: https://www.sciencedirect.com/science/article/pii/S209012 3210000603
- 40. Mukhtar SS, Hassan AS, Morsy NM, Hafez TS, Hassaneen HM, Saleh FM. Overview on Synthesis, Reactions, Applications, and Biological Activities of Schiff Bases. Egypt J Chem. 2021;64(11):6535–48.
- 41. Mohamed S, Karthikeyan S, Ahsin A, Omran O, Mague J, Al-salahi R, et al. Synthesis, Crystal Structure, Computational Investigation of Vanillin Azine Derivative as Potent Blocker of the N- Terminal Ras- Binding Domain (RBD) in Human a- Raf Kinase. ChemistrySelect. 2024 Apr 15;9.
- 42. Essa BM, Sakr TM, Khedr MA, El-Essawy FA, El-Mohty AA. 99mTc-amitrole as a novel selective imaging probe for solid tumor: in silico and preclinical pharmacological study. Eur J Pharm Sci. 2015;76:102–9.
- 43. Fernandes RS, Silva J de O, Lopes SCA, Chondrogiannis S, Rubello D, Cardoso VN, et al. Technetium-99m-labeled doxorubicin as an imaging probe for murine breast tumor (4T1 cell line) identification. Nucl Med Commun. 2016 Mar;37(3):307–12.
- 44. Sakr TM, Moustapha ME, Motaleb MA. 99mTc-nebivolol as a novel heart imaging radiopharmaceutical for myocardial infarction assessment. J Radioanal Nucl Chem. 2013;295(2):1511–6.
- 45. de Barros ALB, Cardoso VN, das Graças Mota L, Leite EA, de Oliveira MC, Alves RJ. A novel d-glucose derivative radiolabeled with technetium-99m: synthesis, biodistribution studies and scintigraphic images in an experimental model of Ehrlich tumor. Bioorg Med Chem Lett. 2010;20(8):2478–80.
- 46. Santos-Cuevas CL, Ferro-Flores G, Arteaga de Murphy C, Ramírez F de M, Luna-Gutiérrez MA, Pedraza-López M, et al. Design, preparation, in vitro and in vivo evaluation of (99m)Tc-N2S2-Tat(49-57)-bombesin: a target-specific hybrid radiopharmaceutical. Int J Pharm. 2009 Jun;375(1– 2):75–83.
- 47. Motaleb MA, El-Safoury DM, Abd-Alla WH, Awad GAS, Sakr TM. Radiosynthesis, molecular modeling studies and biological evaluation of 99mTc-Ifosfamide complex as a novel probe for solid tumor imaging. Int J Radiat Biol [Internet]. 2018;94(12):1134–41. Available from: https://doi.org/10.1080/09553002.2019.1524945
- 48. Essa BM, Sakr TM, Khedr MA, El-Essawy FA, El-Mohty AA. 99mTc-amitrole as a novel selective imaging probe for solid tumor: In silico and preclinical pharmacological study. Eur J Pharm Sci [Internet]. 2015;76:102–9. Available from: http://dx.doi.org/10.1016/j.ejps.2015.05.002